# Promotion of Testa Rupture during Garden Cress Germination Involves Seed Compartment-Specific Expression and Activity of Pectin Methylesterases[1][OPEN]

Claudia Scheler[2], Karin Weitbrecht[2], Simon P. Pearce[2], Anthony Hampstead, Annette Büttner-Mainik, Kieran J.D. Lee, Antje Voegele, Krystyna Oracz, Bas J.W. Dekkers, Xiaofeng Wang, Andrew T.A. Wood, Léonie Bentsink, John R. King, J. Paul Knox, Michael J. Holdsworth[3], Kerstin Müller[3], and Gerhard Leubner-Metzger[3]*

Botany and Plant Physiology, Institute for Biology II, Faculty of Biology, University of Freiburg, D–79104 Freiburg, Germany (C.S., K.W., A.B.-M., K.O., G.L.-M.); Institute of Biochemical Plant Pathology, Helmholtz Zentrum München, Deutsches Forschungszentrum für Gesundheit und Umwelt, D–85764 Neuherberg, Germany (C.S.); Staatliches Weinbauinstitut Freiburg, D–79104 Freiburg, Germany (K.W.); Centre for Plant Integrative Biology (S.P.P., A.H., A.T.A.W., J.R.K., M.J.H.) and Division of Plant and Crop Science (S.P.P., M.J.H., K.M.), School of Biosciences, University of Nottingham, Sutton Bonington Campus, Sutton Bonington, Leicestershire LE12 5RD, United Kingdom; School of Mathematical Sciences, University of Nottingham, University Park, Nottingham NG7 2RD, United Kingdom (S.P.P., A.H., A.T.A.W., J.R.K.); Agroscope, Institute for Plant Production Sciences, Seed Quality, CH–8046 Zurich, Switzerland (A.B.-M.); Centre for Plant Sciences, Faculty of Biological Sciences, University of Leeds, Leeds LS2 9JT, United Kingdom (K.J.D.L., J.P.K.); National Institute for Health Research Trainees Coordinating Centre, Leeds Innovation Centre, Leeds LS2 9DF, United Kingdom (K.J.D.L.); School of Biological Sciences, Plant Molecular Science and Centre for Systems and Synthetic Biology, Royal Holloway, University of London, Egham, Surrey TW20 0EX, United Kingdom (A.V., G.L.-M.); Department of Plant Physiology, Warsaw University of Life Sciences, 02–776, Warsaw, Poland (K.O.); Wageningen Seed Laboratory, Laboratory of Plant Physiology, Wageningen University and Research Centre, NL–6708 PB Wageningen, The Netherlands (B.J.W.D., L.B.); College of Life Sciences, South China Agricultural University, Guangzhou 510642, China (X.W.); and Laboratory of Growth Regulators, Faculty of Science, Palacký University and Institute of Experimental Botany, CZ–783 71 Olomouc, Czech Republic (G.L.-M.)

Pectin methylesterase (PME) controls the methylesterification status of pectins and thereby determines the biophysical properties of plant cell walls, which are important for tissue growth and weakening processes. We demonstrate here that tissue-specific and spatiotemporal alterations in cell wall pectin methylesterification occur during the germination of garden cress (*Lepidium sativum*). These cell wall changes are associated with characteristic expression patterns of PME genes and resultant enzyme activities in the key seed compartments CAP (micropylar endosperm) and RAD (radicle plus lower hypocotyl). Transcriptome and quantitative real-time reverse transcription-polymerase chain reaction analysis as well as PME enzyme activity measurements of separated seed compartments, including CAP and RAD, revealed distinct phases during germination. These were associated with hormonal and compartment-specific regulation of PME group 1, PME group 2, and PME inhibitor transcript expression and total PME activity. The regulatory patterns indicated a role for PME activity in testa rupture (TR). Consistent with a role for cell wall pectin methylesterification in TR, treatment of seeds with PME resulted in enhanced testa permeability and promoted TR. Mathematical modeling of transcript expression changes in germinating garden cress and Arabidopsis (*Arabidopsis thaliana*) seeds suggested that group 2 PMEs make a major contribution to the overall PME activity rather than acting as PME inhibitors. It is concluded that regulated changes in the degree of pectin methylesterification through CAP- and RAD-specific PME and PME inhibitor expression play a crucial role during Brassicaceae seed germination.

Mature seeds of members of the Brassicaceae family such as Arabidopsis (*Arabidopsis thaliana*) and garden cress (*Lepidium sativum*) are endospermic (i.e. the embryo is surrounded by a thin living cell layer, the endosperm, and a dead outer layer, the testa). Many angiosperm seeds, including those of garden cress and Arabidopsis, germinate in a two-step process: after the initial phase of water uptake by the dry seeds (imbibition), testa rupture (TR) occurs and is subsequently followed by endosperm rupture (ER), which marks the completion of germination (Liu et al., 2005; Müller et al., 2006). Germination is controlled by two opposing forces, the increasing growth potential of the radicle and the resistance of the testa and endosperm tissues covering it (Bewley, 1997; Schopfer, 2006; Linkies and Leubner-Metzger 2012). After TR, endosperm resistance decreases through tissue softening, a process called endosperm weakening (Müller et al., 2006; Linkies et al., 2009). Both radicle elongation and endosperm weakening require cell wall modifications (Schopfer, 2006; Müller et al., 2009; Morris et al., 2011).

Plant cell walls are the main determinants for the shape and biomechanical properties of plant tissues,

organs, and even the whole plant body. They control turgor-driven water uptake to allow cell growth through changes in extensibility, which depend on wall composition and the interaction between their components (Thompson, 2005; Cosgrove and Jarvis, 2012; Yoshida et al., 2014). One of the most abundant groups of polysaccharides in primary cell walls is pectins. Pectins are complex polysaccharides that are characterized by $\alpha$-1,4-linked galacturonic acid (Willats et al., 2001; Mohnen, 2008; Tan et al., 2013); they are present in the middle lamellae and are key polymers in cell separation processes. The most abundant plant cell wall pectin is homogalacturonan (HG). HG is a linear polymer of (1,4)-linked-$\alpha$-D-galacturonic acid that can be modified by methylesterification at the C-6 carboxyl position to form methylesterified homogalacturonan (Me-HG; Wolf et al., 2009a). The degree of methylesterification is variable between developmental stages, tissues, and even regions of the wall of an individual cell and strongly affects the mechanical properties of cell walls (Braybrook et al., 2012). After synthesis in the endomembrane system, HG is secreted in a highly methylesterified form into the plant cell wall of growing cells (Mohnen, 2008).

Pectin methylesterases (PMEs; EC 3.1.1.11) catalyze the demethylesterification of HG (Wolf et al., 2009a). PMEs are ubiquitous cell wall-associated enzymes that are found in all higher plants as well as in some bacteria and fungi. PMEs can act linearly to deesterify stretches of Me-HG to give rise to blocks of free carboxyl groups that can be cross-linked by calcium ions. These calcium bridges influence cell wall porosity and may enhance the overall firmness of tissues. PMEs also can act in a nonlinear fashion and deesterify only individual galacturonate residues or short stretches, which does not allow for calcium bridges to form, leading to a looser cell wall matrix structure. PME activity might promote the subsequent action of cell wall hydrolases such as endopolygalacturonases (Wakabayashi et al., 2000, 2003),

which contribute to cell wall weakening and/or cell separation (González-Carranza et al., 2007). PMEs have been shown to be involved in pectin remodeling at different developmental stages, such as pollen tube growth (Eckardt, 2005), root elongation and its reaction to soil aluminum concentrations (Yang et al., 2013), hypocotyl elongation (Pelletier et al., 2010), fruit ripening (Hyodo et al., 2013), and seed germination (Müller et al., 2013). PMEs are encoded by a large multigene family that has been classified into two groups (Wang et al., 2013): all PMEs have a conserved pectinesterase domain (Pfam01095), but only group 2 has in addition a PME inhibitory domain (Pfam04043). PME activity is regulated by pectin methylesterase inhibitor (PMEI) proteins (Giovane et al., 2004; Wolf et al., 2009a).

In our integrative study, we discovered that during the seed germination of garden cress, changes in the transcript abundance of specific PMEs and PMEIs are reflected in seed compartment-specific changes in PME activity and accompanied by spatiotemporal changes in cell wall pectin methylesterification. We mathematically modeled the contribution of the different groups of PMEs and of PMEIs to the degree of methylesterification in the garden cress seed cell walls. Based on these molecular, physiological, histochemical, and biophysical analyses, we propose that PME activity is involved in the germination process of garden cress and is differentially regulated in a spatial and temporal manner.

## RESULTS

### Seed Compartment-Specific Transcriptome Analysis of Garden Cress Germination

We utilized the fact that garden cress has a two-step germination process, with TR and ER separated by several hours, to conduct a dense spatiotemporal transcriptome analysis during the germination process (Fig. 1). We investigated transcriptome changes in the seed compartments that are directly involved in ER, the micropylar endosperm (CAP; Fig. 1B) and the radicle with the lower part of the hypocotyl (RAD; embryo growth zone; Fig. 1B), at key time points during the germination process from early imbibition to the completion of ER (Fig. 1, A and B). At the time points when approximately 50% of the seed population had reached TR and ER, respectively, we divided the sampling population between the seeds that had already undergone rupture (+TR or +ER) and those that had not (−TR or −ER), so that we could compare samples that would have undergone TR within the next 1 or 2 h with those that already had ruptured testas. We also sampled cotyledons (COTs) and nonmicropylar endosperms (NMEs) at three time points (Fig. 1). Seed compartment-specific gene expression analyses for garden cress have been performed successfully before (Linkies et al., 2009) using Complete Arabidopsis Transcriptome Microarray-spotted PCR-amplified gene-specific tag-based chips, but only for a small number of samples that allowed for a
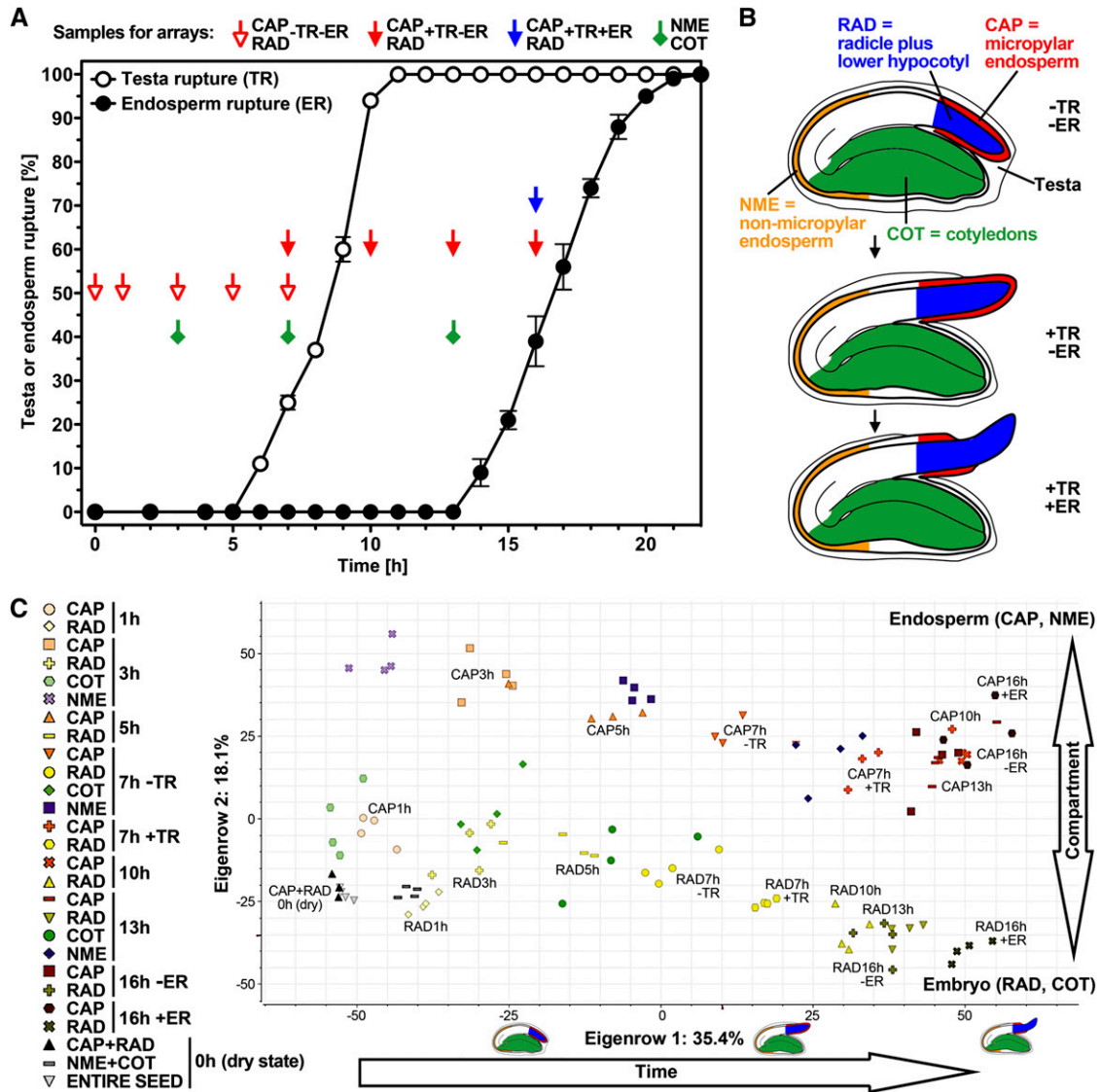
**Figure 1.** Spatiotemporal transcriptome analysis of garden cress 'FR14' seed compartments during germination. A, The kinetics of garden cress TR and ER at 24°C in continuous light. Arrows indicate sampling time points for RNA extraction at which the seeds were dissected into CAP, RAD, COT, and NME, as indicated. Note that at 0 h (dry seed stage), CAP plus RAD as well as NME plus COT were sampled together. Mean values ± SE of $n = 4$ plates each with 100 seeds are presented for TR and ER. B, Garden cress seed compartments (CAP, RAD, COT, and NME) at different stages during germination as related to the TR and ER kinetics. C, Principal component analysis (PCA) of the garden cress microarray results with four biological RNA replicates for each time point. Eigenrow 1 separates transcriptomes in time, while eigenrow 2 separates the seed compartments.

limited analysis of the garden cress germination process. Our sampling concept in this work with garden cress (Fig. 1) led to a time course with sufficient spatiotemporal resolution to investigate the distinct phases of germination and make physiologically relevant comparisons.

We performed microarrays by hybridizing garden cress RNA to Affymetrix ATH1 microarrays designed for Arabidopsis. Heterologous microarrays on Arabidopsis ATH1 chips have been employed successfully by several groups to elucidate transcriptome changes in unsequenced Brassicaceae species or in species without commercially available microarrays (Hammond et al., 2006; Slotte et al.,

2007). To further improve the method for garden cress, we developed a sophisticated masking approach that allowed us to extract a maximum of information from the arrays (see "Materials and Methods"). Using the masking method presented here, with a false discovery rate of 0.01, 36.6% of probes and 65.1% of probe sets were retained, leading to 5,793 genes identified as being differentially expressed between 1 and 16 h after sowing in the CAP, and 6,098 genes in the RAD. Conversely, using the method of Hammond et al. (2005), the maximal number of differentially expressed genes was 1,712 at a cutoff of 100. Thus, our method retained a much larger number of differentially

expressed genes that could then be used for further analysis. Therefore, normalized expression values for garden cress were obtained for 13,895 transcripts (Supplemental Data Set S1), with garden cress gene transcripts referring to the putative Arabidopsis orthologs defined by having an Arabidopsis Genome Initiative identifier such as At1g62380. Supplemental Data Sets S2 and S3 provide the normalized log$_2$ values for the mean and SD expression results, respectively.

## Seed Compartment-Specific Differentially Regulated Garden Cress Transcriptome during Germination Shows Overrrepresentation of Cell Wall-Related Transcripts at the TR Stage Transition

A principal component analysis (PCA) shows the general distribution of values calculated into eigenvectors and makes it possible to identify the eigenvectors with the greatest influence on sample variance. In our arrays, the eigenvectors with the biggest influence appear to correspond to time and seed compartment (Fig. 1C). In dry seeds and at 1 h after sowing, RAD and CAP samples still cluster together, separating from 3 h after sowing. In the RAD, distinct clusters formed at the phase transition time point at 7 h, where we segregated for −TR and +TR, and at 16 h, where we segregated for seeds that had undergone ER and thus completed the germination process (+ER) and those whose endosperm had not ruptured yet (−ER). The same was true for the CAP at 7 h (+TR versus −TR), although the 16-h CAP with ER clusters with the CAP samples without ER.

The COT samples exhibited a higher variance throughout the time course (Fig. 1). The NME for the two time points without TR clustered apart from the CAP samples but was still closer to them than to the RAD and COT samples derived from the embryo. At 13 h, the NME samples varied more and clustered closer still to the CAP samples (Fig. 1). The finding that transcriptomes differ between the distinct seed compartments and over time is further supported by a cluster analysis of the transcript abundance patterns, which showed five clearly distinct clusters (Supplemental Fig. S1). Together with the principal component analysis (Fig. 1), it supports the view that TR is a decisive step during the germination process that is associated with abundant transcriptomes changes (+TR versus −TR) in both the CAP and the RAD.

The Gene Ontology (GO) overrepresentation analyses of the TR rupture transition time point (Supplemental Tables S1 and S2) indicate that both hormone regulation and cell wall modifications are overrepresented in the differentially regulated transcripts in the different seed compartments. We decided to look in more detail at PME and PMEI, as those cell wall-modifying enzymes and inhibitors have been shown to be tied in with hormonal regulations and to play a role in seed germination of Arabidopsis (Müller et al., 2013; Saez-Aguayo et al., 2013), and pectinesterase activity and inhibition was one of the activities whose GO terms were specifically overrepresented in the RAD (Supplemental Table S2).

## Spatiotemporal Patterns of HG and Me-HG Pectin Cell Wall Epitopes during Garden Cress Seed Germination

In order to observe if, where, and at which stage during the garden cress seed germination process changes in the degree of pectin methylesterification actually happen in the RAD and CAP, we studied HG epitopes in situ. To distinguish pectic HG in its methylesterified form (Me-HG) from the demethylesterified form (HG), we used a set of well-characterized monoclonal antibodies (www.plantcellwalls.net) in conjunction with fluorescence imaging (Fig. 2). Antibody LM19 is specific for demethylesterified HG, and its epitope was detected in seeds 3 h after sowing. The LM19 epitope was ubiquitously distributed in the cell walls of the RAD as well as in the CAP (E in Fig. 2), the testa, and the testa-derived mucilage layer. In contrast, the JIM7 (Fig. 2) and LM20 (data not shown) Me-HG epitopes were restricted to the testa and mucilage and were present at reduced levels in the RAD but absent from the CAP. The pattern of the LM19 HG epitope did not change between our sampling times. However, the spatial distribution of Me-HG (JIM7) was altered. The JIM7 signal increased in the RAD and appeared in the inner cell wall of the CAP upon TR (Fig. 2). This suggests that there is new deposition of pectin into the cell wall, as HG is methylesterified in the Golgi and secreted as Me-HG. In testa and mucilage, the JIM7 epitope was detectable in all phases during seed germination (Fig. 2).

## Molecular Phylogenetic Analyses of Arabidopsis and Garden Cress PMEs and Their Inhibitors

We mined our microarrays for the expression patterns of putative PMEs and PMEIs in garden cress seeds (Supplemental Data Sets S1–S3). As the garden cress genome has not been sequenced, we started by identifying 136 Arabidopsis sequences for PMEs and PMEIs by annotation and similarity searches in public databases, with subsequent verification of the existence of specific domains in the predicted proteins. According to our molecular phylogenetic analysis of their full-length predicted protein sequences, these Arabidopsis PMEs and PMEIs cluster into three large groups (Fig. 3): group 1 PME (22 members) and group 2 PME (45 members) contain the PME domain (Pfam01095), which harbors five characteristic sequence motifs important for PME activity. The group 2 PMEs additionally possess a PMEI domain (Pfam04043) with conserved Cys residues, and both domains are separated by a processing motif that is a putative target for subtilisin-like proteases. The third cluster consists of 69 PMEIs (Fig. 3).

We used the seed-specific Electronic Fluorescent Pictograph browser and the eNorthern tool at www.bar.utoronto.ca (Winter et al., 2007) for an in silico analysis of the PME/PMEI transcript expression patterns in imbibed whole Arabidopsis seeds (Fig. 3). This analysis yielded a general pattern in which many PME group 2 transcripts are down-regulated by cold stratification (1 in Fig. 3). However, a small number of group 2 PMEs
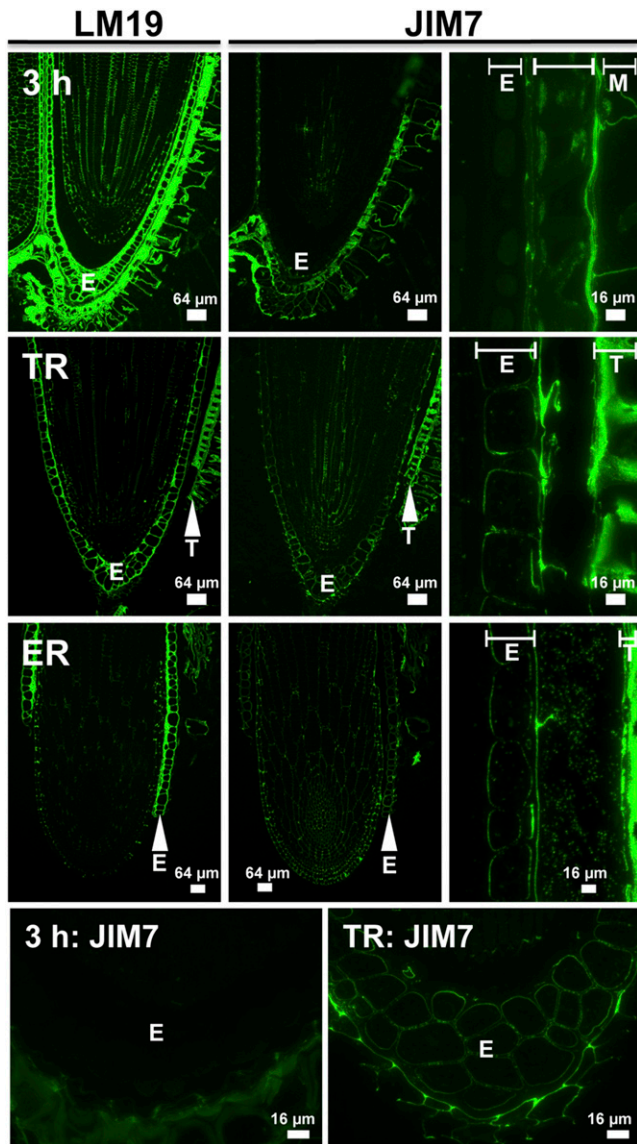
**Figure 2.** Immunolocalization of the LM19 HG and JIM7 Me-HG pectin cell wall epitopes in longitudinal sections of germinating garden cress seeds 3 h after imbibition (3 h), at TR, and at ER. Immunodetection with LM19 indicates the ubiquitous distribution of HG in all cell walls of the embryo, the endosperm (E), at the testa surface (T), and in mucilage (M). By contrast, immunodetection with JIM7 indicates that the occurrence of Me-HG is restricted to the mucilage and testa surface, with reduced levels detectable in the radicle at 3 h. Comparative high-magnification micrographs of endosperm tissue at 3 h indicate the absence of the JIM7 epitope and its appearance in endosperm cell walls by TR, suggesting the deposition of newly synthesized HG. Arrowheads with E and T indicate ruptured endosperm and testa, respectively.

and PMEIs was strongly up-regulated during the first few hours of the germination process (2 in Fig. 3). PMEs from both groups as well as PMEIs are up-regulated in the course of the germination process in the presence of abscisic acid (ABA; 3 in Fig. 3).

We then compared the expression of PME and PMEI transcripts that we identified in our arrays for garden cress seeds (four group 1 PMEs, 28 group 2 PMEs, and 25 PMEIs) in CAP and RAD (Fig. 4) with their homologs in Arabidopsis (data extracted from the transcriptome of Dekkers et al. [2013]) as defined by the transcripts that bind to the same probe sets. There was an overall stronger differential regulation visible in the Arabidopsis data, which may be due to the heterologous nature of the garden cress arrays or to the fact that the Arabidopsis seed compartments were less confined and contained additional tissues (Fig. 4). However, we could clearly observe that the genes that were strongly differentially regulated in garden cress seed compartments were also strongly regulated in Arabidopsis in a similar manner in the same compartments (Fig. 4).

## PME Activity in Garden Cress Seed Compartments in Relation to TR and ER

With the large number of PMEs and PMEIs and their diverse expression patterns, it is hard to predict whether there is a net PME activity at any given stage and seed part and how it changes over the course of germination. Therefore, we measured the total PME activity in garden cress RADs and CAPs. The total PME enzyme activity was roughly 10-fold higher in the CAP compared with the RAD during garden cress seed germination (Fig. 5). The PME activities in the CAP were highest during imbibition and in the very early phase of germination (3–8 h), declined around the time of TR, and then stabilized at a lower activity as the population reached the completion of TR followed by ER (16 h; Fig. 5A). The activity in the RAD also decreased around TR, then increased again as the seeds neared ER, and peaked at a stage where the whole population had reached TR but not yet progressed to ER (16 h).

Endosperm weakening and rupture of garden cress are known to be delayed by exogenous ABA, while the kinetics of TR is unaffected by its presence. In accordance with this, when ABA was added to the germination medium, the population only completed ER after about 70 h, but the timing of TR did not change significantly (Fig. 5B). PME activity in the CAP during the early germination phase before TR was similar in seed populations with and without ABA. However, when this seed population neared its delayed ER, PME activity was significantly lower than at the physiologically equivalent time point without ABA (Fig. 5B). PME activity in the RAD was relatively constant over time and approximately 2-fold lower in the ABA series compared with the control (Fig. 5B).

## Mathematical Model of PME Activity in the Garden Cress CAP and RAD

As mentioned above, PMEs fall into two groups, one of which (group 2) contains a PMEI domain. In order to explore the significance of the two PME groups, along with the action of the PMEIs, on the total PME activity and, therefore, to the pectin demethylesterification process, we
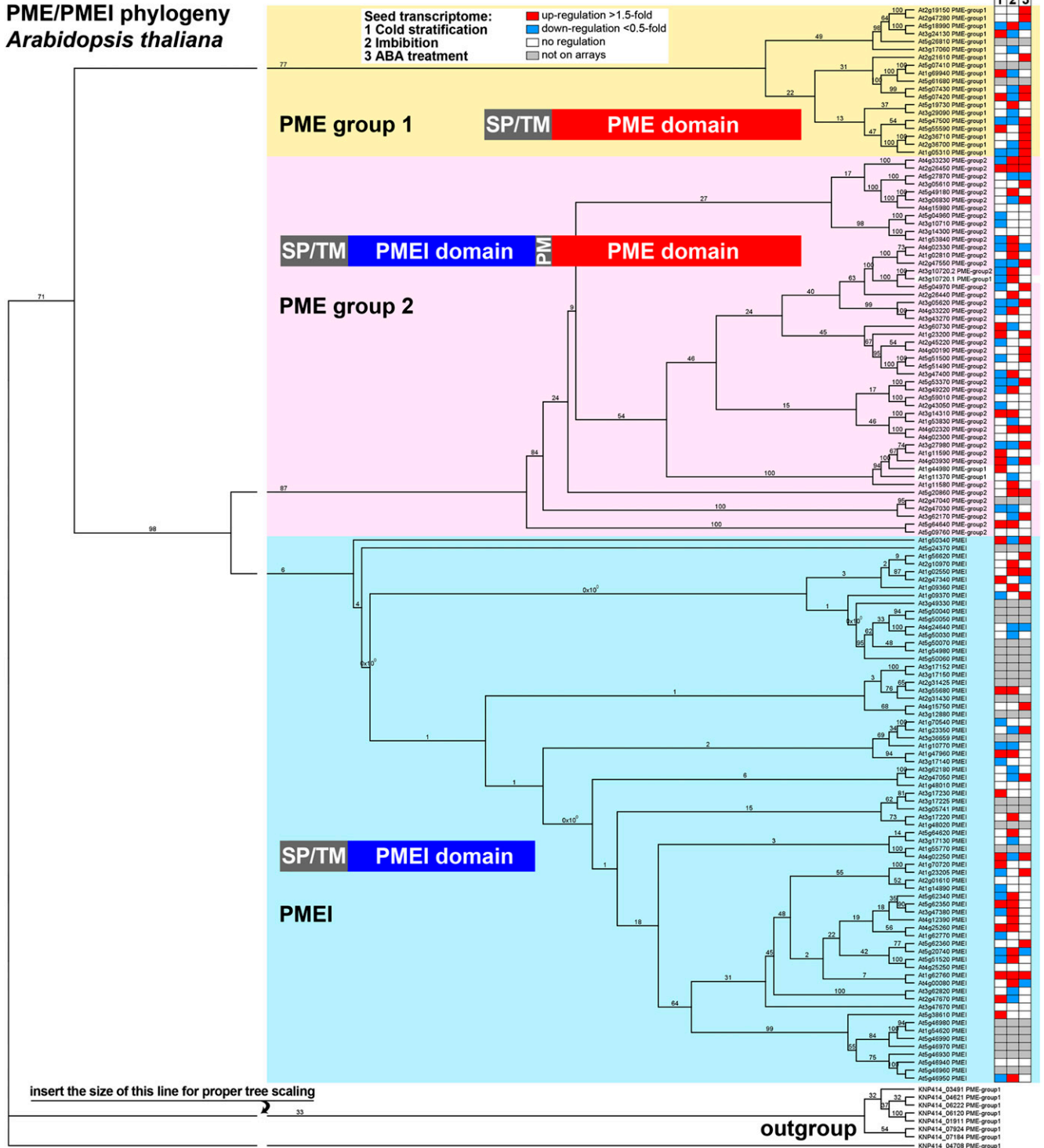
**Figure 3.** Phylogeny of Arabidopsis PMEs and PMEIs and transcript expression in germinating seeds. Phylogenetic analysis of the predicted full-length amino acid sequences of 136 PMEs and PMEIs (Supplemental Data Set S4) reveals three distinct phylogenetic groups: PME group 1 (yellow) with a specific PME domain; PME group 2 (rose) with a PME domain and an inhibitory domain; and PMEI (blue) with just the inhibitory domain. We used the MUSCLE algorithm for the amino acid multiple sequence alignment, and a maximum likelihood tree was constructed using PYHML. A similar tree topology (i.e. the same major clusters and subclusters) was also obtained when a different alignment algorithm was used (MAFFT). We used several PMEs of *Paenibacillus mucilaginosus* as an outgroup. Note that in our phylogenetic analysis, three sequences of PME enzymes without PMEI domains are localized within PME group 2 (highlighted with white background) due to the high similarity of their

constructed a biologically informed network of reactions (Fig. 6A) and converted it into a system of ordinary differential equations. Cumulative transcript accumulation for each PME group (Fig. 6B) was used as a proxy for their protein accumulation. The network (Fig. 6) that was used as a basis for our set of ordinary differential equations centers on the demethylesterification of Me-HG, caused by either of the PME groups, with PMEI inhibiting both groups of PMEs and group 2 PMEs able to inhibit themselves. Several assumptions were made to simplify the system for the purpose of modeling: (1) spatial variations are neglected; (2) negligible deposition of additional pectin occurs over the time scale of interest (germination process until approximately 16 h); (3) interactions between PME proteins and their inhibitors irreversibly remove the proteins from the system; (4) protein production rates are proportional to the levels of the relevant mRNA, the latter being obtained from the transcriptomic data; and (5) a group 2 PME molecule is able to inactivate itself, since it contains both the PME and PMEI domains. These assumptions and the network (Fig. 6A) lead to Equations 1 to 8 (Fig. 6C); for further explanation, see "Materials and Methods." The model was fitted to the PME enzyme data shown in Figure 5A, with the resulting parameters listed in Supplemental Table S3. The resulting PME activity predicted by the model after fitting is shown in Figure 6D in comparison with the measured PME enzyme activity data.

PME and PMEI cumulative transcript accumulation within garden cress seed compartments, our proxy for protein production, appears to be phasic in both CAP and RAD (Fig. 6B): first, the group 1 PMEs are produced, then the PMEI proteins, and finally the group 2 PMEs. This is especially striking in the RAD, since the group 2 PMEs do not have the same escalation in the CAP, where group 2 PME production peaks around the time of TR before declining. Parameter sensitivity analysis was carried out on the model, and it was noted that altering the activating reaction rate, $\alpha_i$, has a greater impact on the model than varying the inhibiting reaction rate, $\zeta_i$. Therefore, our parameter (Supplemental Table S3) sensitivity analysis gives insight into which processes are most significant in governing the overall activity and open the way for subsequent application of the model and for its refinement.

Our mathematical model implies that inhibiting processes, in particular by the group 2 PMEs, are less important for the overall activity than their demethylesterification function. This suggests that the primary importance of the group 2 PMEs is in their PME action rather than their PMEI behavior (see "Discussion"). Therefore, analyzing the group 2 PME expression pattern (see below) is relevant to the PME enzyme activity pattern (Fig. 5).

## Hormonal and Seed Compartment-Specific Regulation of Garden Cress Group 2 PMEs

With the large number of differentially regulated group 2 PMEs (Fig. 4) in our arrays for both RAD and CAP, as well as the insight from the model (Fig. 6) that the group 2 PMEs are predicted to play a role mostly as PMEs and not as inhibitors, we decided to clone and look in detail at several garden cress group 2 PMEs (Fig. 7). Several group 2 PMEs were dramatically up-regulated in whole Arabidopsis seeds (Fig. 3): *At1g11580* increased more than 100-fold, but we did not obtain data corresponding to this transcript from our heterologous array analysis. *At2g26440* and *At3g14310* were more than 100-fold up-regulated during the first 24 h of imbibition in Arabidopsis, but they did not show changes in the *L. sativum* arrays in either seed compartment under the conditions we used for our arrays.

We fully cloned and analyzed the complementary DNAs (cDNAs) for the garden cress PME group 2 homolog of Arabidopsis *At1g11580*, which we named *LesaPME11580*. All other cloned garden cress PME cDNAs were named following the same principle, including PME group 2 *LesaPME26440*, *LesaPME14310*, and *LesaPME51490* (Supplemental Table S4). Taken together, the sequence comparisons (for details, see Supplemental Fig. S2) considering known domains (Markovic and Janecek, 2004; Pelloux et al., 2007) strongly suggest that *LesaPME11580* is a functional PME group 2 of garden cress. We also cloned the full-length cDNA of *LesaPMEI14890*, which shows the typical PMEI domain and other characteristic features of this class of inhibitors (Supplemental Fig. S2), and therefore is most likely a functional PMEI.

Using quantitative real-time reverse transcription (qRT)-PCR, we analyzed the transcript expression of the garden cress group 2 PMEs (Fig. 7) and a small selection of group 1 PMEs and PMEIs (Supplemental Fig. S3) in the CAP and RAD with and without exposure to ABA. In vitro PME activities were measured in the CAP and RAD at two sampling time points, seeds that had just undergone TR (Early $ER_{0\%}$) and seeds just before ER (Late $ER_{50\%}$), for the control and ABA treatments (Fig. 7A). In all conditions tested,

---

**Figure 3.** (*Continued.*)
PME domains to the PME domain of group 2. One of these three PMEs, At3g10720, generates two different RNAs by alternative splicing. If both RNAs are translated, they would produce a group 1 PME (At3g10720.1) and a group 2 PME (At3g10720.2) protein. Columns at the right next to the Arabidopsis Genome Initiative numbers show results from eNorthern analysis for Arabidopsis seed cold stratification (1), imbibition (2), and ABA treatment (3); red indicates up-regulation, blue indicates down-regulation, and white indicates no regulation in entire seeds. Gray genes are not present in the data sets used. The transcriptome analysis is available via the seed-specific Electronic Fluorescent Pictograph browser at www.bar.utoronto.ca, on which this analysis was based, with nondormant, after-ripened wild-type seeds. Structural motifs are according to Pelloux et al. (2007): PM, processing motif; SP, signal peptide; TM, transmembrane domain.
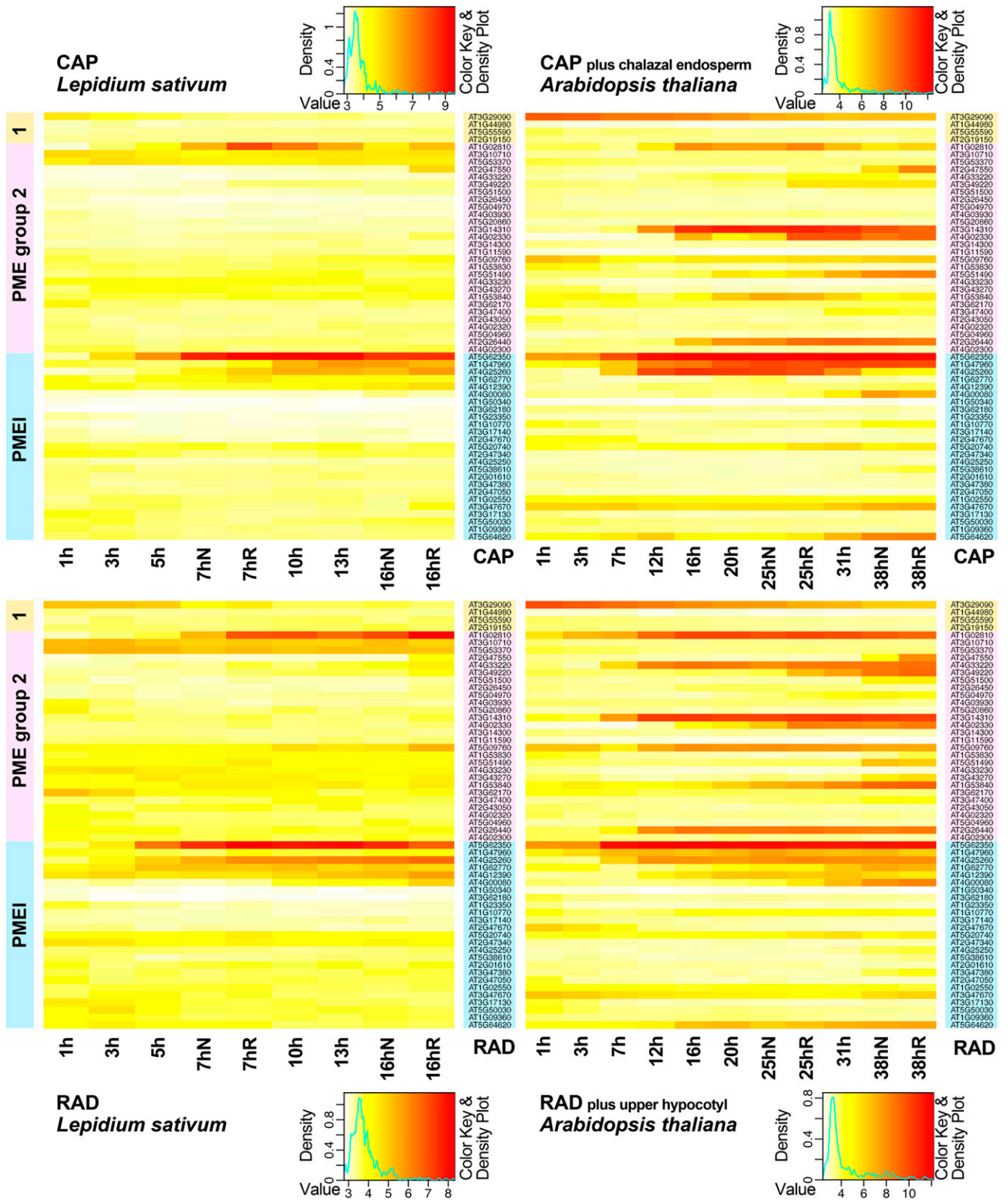
**Figure 4.** Seed compartment-specific expression patterns of PMEs and PMEIs in garden cress and Arabidopsis. At top, heat maps show the expression patterns of PME and PMEI transcripts in our microarrays of the garden cress CAP (left) compared with the expression of the putative ortholog in the Arabidopsis CAP plus chalazal endosperm (right). At bottom, the expression patterns of PME and PMEI transcripts in our microarrays of the garden cress RAD (left) are compared with the expression patterns of the

PME activity in the RAD was significantly lower than in the CAP. In both seed compartments, ABA inhibited PME activity compared with the untreated control (Fig. 7A). Supplemental Figure S3 contains additional data for exposure to 1-aminocyclopropane-1-carboxylic acid (ACC), the precursor of the plant hormone ethylene, which acts antagonistically to ABA in the germination process of garden cress (Linkies et al., 2009). ACC had no effect on total activity in the presence or absence of ABA in the RAD but led to a strong increase in activity in the CAP at the TR time point (Supplemental Fig. S3).

All transcripts we investigated showed a response to ABA that differed between RAD and CAP, confirming the importance of investigating the seed compartments separately. *LesaPME11580* was expressed more abundantly in the RAD compared with the CAP (Fig. 7B). The transcript stayed at the same level at the two time points we investigated in the RAD but declined in the CAP between the early and late time points. Treatment with ABA down-regulated *LesaPME11580* in all conditions tested and in both seed compartments (Fig. 7B), while ACC caused a down-regulation only in the CAP and not in the RAD (Supplemental Fig. S3). In situ mRNA hybridization (Supplemental Fig. S4) confirmed that *LesaPME11580* transcripts localized to the RAD and were hardly detectable in the CAP. *LesaPME26440* was also predominantly expressed in the RAD (Fig. 7C), but contrary to *LesaPME11580*, it was down-regulated in the presence of ABA specifically at the early time point in the CAP and the late time point in the RAD. In addition, its abundance in the CAP was lower at the later time point than it was at the early time point. *LesaPME51490* showed a predominant expression in the CAP (Fig. 7D), while *LesaPME14310* was expressed in both seed compartments at a low level (Fig. 7E). *LesaPME14310* expression was sensitive to ABA in the medium only at the late time point in the RAD, whereas ABA had no effect on *LesaPME14130* at the other time points. Compared with the four group 2 PMEs that we investigated, the group 1 *LesaPME29090* transcript abundance was around 10-fold higher, and there was no appreciable down-regulation by ABA (Supplemental Fig. S3).

## Exogenous Treatment with PME Enhances Testa Permeability and Promotes TR

Having investigated the endogenous PME transcript abundances, activities, and pectin methylesterification patterns in the garden cress CAP and RAD during germination, we focused on the question of whether treatment of seeds with exogenous PME affects their germination. Interestingly, addition of 0.2 units of orange (*Citrus sinensis*) peel PME to the seed incubation medium (0.03 units PME mL$^{-1}$) promoted their TR (Fig. 8A) but did not appreciably affect ER (Supplemental Fig. S5A). In contrast, relatively high PME amounts (approximately 20 units) delayed TR and ER (Supplemental Fig. S5). Earlier work (Linkies et al., 2009) showed that, while treatment of garden cress seeds with ABA or the ethylene precursor ACC affected ER, it did not affect the kinetics of TR. Addition of 0.2 units of PME plus ABA or ACC to the seed incubation medium also promoted TR (Fig. 8A), which suggests that the PME action is a direct effect of the enzyme action and could be associated with an increased testa and/or mucilage permeability.

To assay for testa permeability, we imbibed seeds in tetrazolium assay solution, a method used to analyze Arabidopsis *transparent testa* mutants (Debeaujon et al., 2000) and the effect of myrigalone A on garden cress seeds (Voegele et al., 2012). We imbibed garden cress seeds in tetrazolium salt solution in the absence (CON) or presence of 0.2 units of PME, thus at a concentration of PME that led to earlier TR. After 9 h, the embryos were excised from the seeds, photographed, and categorized (Fig. 8B). For CON, 88% of the embryos were unstained (i.e. the testa was impermeable to the dye) and 12% were yellow, showing a low staining intensity that indicates the low testa permeability. Thus, the testa permeability of CON-imbibed seeds for tetrazolium salts was very low. In contrast, for seeds treated with 0.2 units of PME, only 46% of the embryos were pale (impermeable) and 20% stained yellow (low permeability), while 34% stained partly (either at the COT base or the radicle tip) or almost fully red (highly permeable; Fig. 8B; Supplemental Fig. S6).

PME-mediated demethylesterification of Me-HG increases the cell wall HG content. Polygalacturonase (PG) is a pectin-degrading enzyme that cleaves the $\alpha$-1,4-D-galacturonosidic linkages of HG chains. Concerted action of PME and PG, therefore, is known to cause extensive pectin depolymerization (Wakabayashi et al., 2000, 2003). Therefore, we assumed that, if testa and mucilage permeability depend on the state of pectin, PG should further enhance the testa permeability when exogenously applied in combination with 0.2 units of PME. This was indeed the case: only 18% of the embryos were pale (impermeable), 20% were stained yellow, and 62% were stained partly or almost fully red upon treatment with PME plus PG (Fig. 8B; Supplemental Fig. S6). We conclude that the promoting effect on TR and ER by low concentrations of PME is at least partially achieved through an enhanced permeability of the testa and/or mucilage layer (Fig. 8).

**Figure 4.** (*Continued.*)
putative Arabidopsis ortholog in the Arabidopsis RAD (right). The Arabidopsis results were extracted from the microarray database published by Dekkers et al. (2013). Note that, in contrast to garden cress (Fig. 1B), the Arabidopsis CAP compartment contains the chalazal endosperm in addition to the micropylar endosperm and the Arabidopsis RAD compartment contains the upper hypocotyl in addition to the lower hypocotyl (embryo growth zone) and radicle (Dekkers et al., 2013).

## DISCUSSION

### TR Constitutes a Transition between Phases of Gene Expression and Enzyme Activities in the Garden Cress CAP and RAD

Our microarray analysis provides a high-resolution picture of seed compartment-specific transcriptome changes during garden cress seed germination. The added density of sampling time points made possible by this technical advance supports the identification of the importance of TR as a transitional event during garden cress seed germination. Many transcripts showed an increase in abundance shortly before or more often just after the TR event. One group of genes strongly up-regulated around TR are cell wall-modifying enzymes, and cell wall-related genes were evident in our GO over-representation analysis. This indicates the importance of
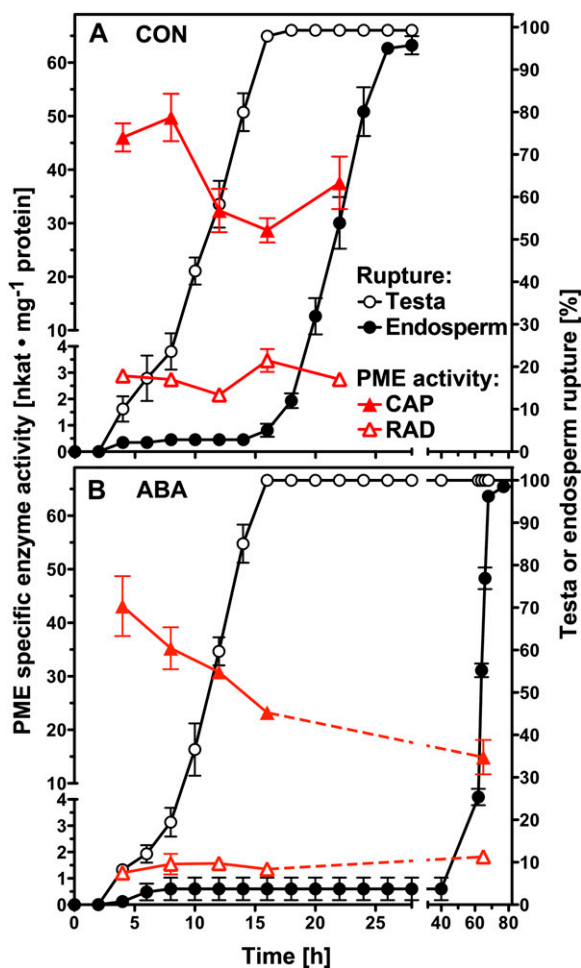


**Figure 5.** PME enzyme activity during the seed germination of garden cress. Seeds were imbibed in water (control [CON]; A) or 5 μM ABA (B). The kinetics of garden cress TR and ER at 18°C in continuous light is shown. PME enzyme activity was measured for protein extracts of CAP and RAD excised from imbibed seeds at the times indicated. Mean values ± SE for four biological replicates with 100 seeds each are presented.
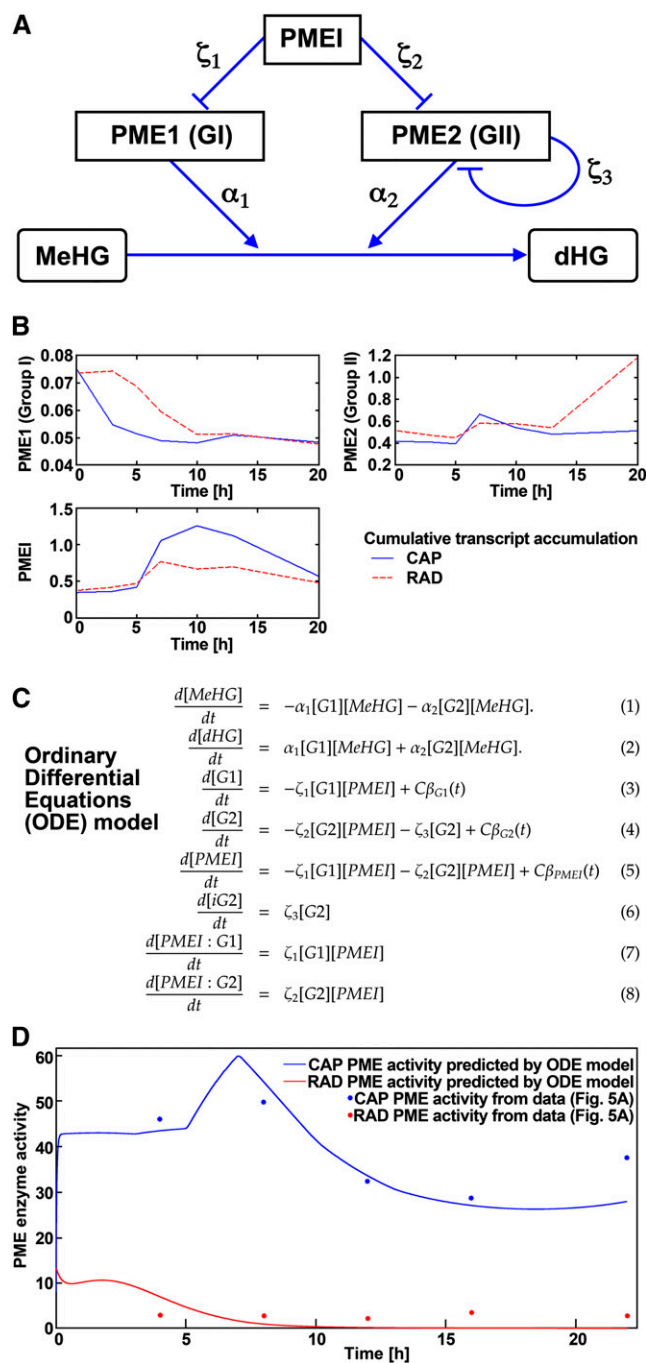


$$\frac{d[MeHG]}{dt} = -\alpha_1[G1][MeHG] - \alpha_2[G2][MeHG]. \quad (1)$$

$$\frac{d[dHG]}{dt} = \alpha_1[G1][MeHG] + \alpha_2[G2][MeHG]. \quad (2)$$

$$\frac{d[G1]}{dt} = -\zeta_1[G1][PMEI] + C\beta_{G1}(t) \quad (3)$$

$$\frac{d[G2]}{dt} = -\zeta_2[G2][PMEI] - \zeta_3[G2] + C\beta_{G2}(t) \quad (4)$$

$$\frac{d[PMEI]}{dt} = -\zeta_1[G1][PMEI] - \zeta_2[G2][PMEI] + C\beta_{PMEI}(t) \quad (5)$$

$$\frac{d[iG2]}{dt} = \zeta_3[G2] \quad (6)$$

$$\frac{d[PMEI:G1]}{dt} = \zeta_1[G1][PMEI] \quad (7)$$

$$\frac{d[PMEI:G2]}{dt} = \zeta_2[G2][PMEI] \quad (8)$$

**Figure 6.** Mathematical model of the contributions of group 1 PMEs, group 2 PMEs, and PMEIs to overall PME activity in RAD and CAP during garden cress seed germination. A, Network diagram, where $\alpha_i$ indicates the rates at which Me-HG is demethylesterified and $\zeta_i$ represents the rates at which a PMEI domain binds with a PME domain. dHG, Demethylesterified HG. B, Plots of the $\beta$-functions: cumulative transcript levels for each group within the CAP and RAD of garden cress during germination; these levels are used as approximations of protein production. C, Ordinary differential equations based on our network model and the law of mass action. D, Predicted PME activities when using the garden cress PME model and fitting to the garden cress data (Fig. 5A) for PME enzyme activity within the CAP and RAD. For a detailed description of the modeling, see "Materials and Methods"; for the parameter values for the mathematical model, see Supplemental Table S3.
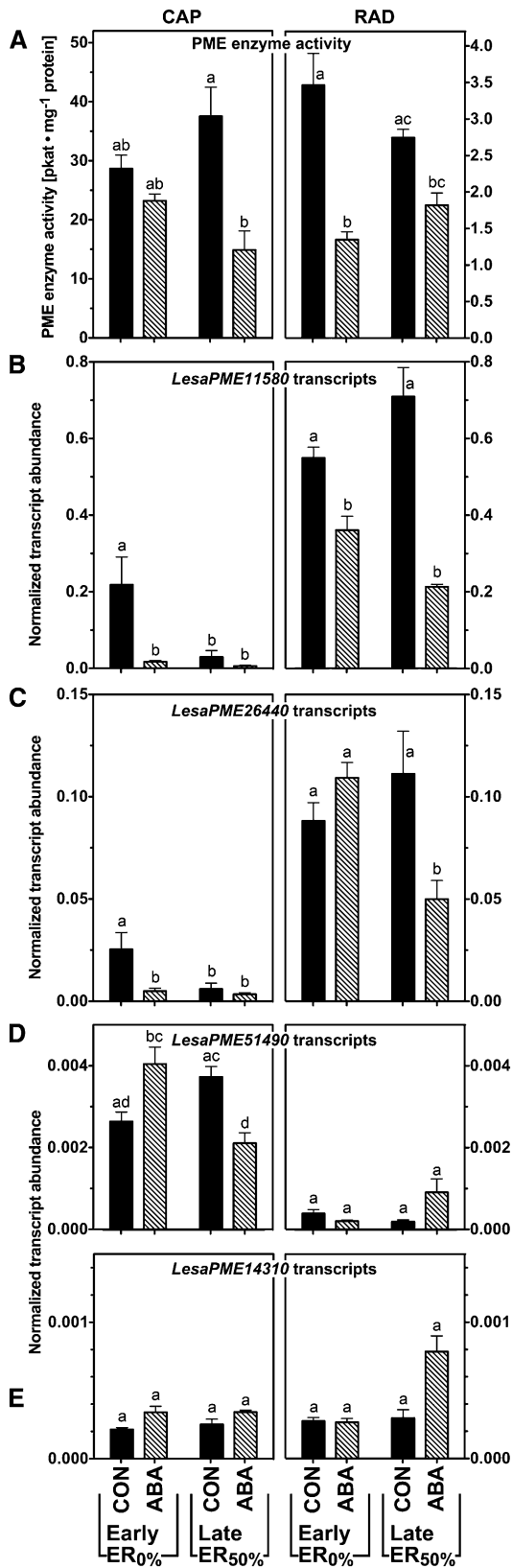
**Figure 7.** Spatial and temporal analysis of transcript abundances of novel garden cress (*Lesa*) group 2 PMEs in germinating seeds (18°C and continuous light) by qRT-PCR. A, PME enzyme activities as determined

cell wall remodeling in the CAP and RAD around and after the time of TR. This increased level of expression is then maintained or further increased for the remaining germination process. While specific groups of genes such as the cell wall-modifying enzymes are up-regulated at TR, the overall number of differentially regulated genes drops drastically once TR is complete. These observations fit with those made using microarrays with seed compartment-specific RNA of Arabidopsis, where TR also emerged as a central event for transcriptional regulation in seeds (Dekkers et al., 2013). The transitional nature of the TR time point was also evident in our principal component analysis (Fig. 1): up to and including TR, the CAP and NME endosperm samples are clearly distinguishable, but after TR from 10 to 16 h with and without ER, the samples cluster together as one group.

As TR is not influenced by the presence of ABA in the germination medium, but ER is strongly delayed by ABA, and the processes that begin at TR are clearly subject to further hormonal regulation once they have been initiated (Linkies et al., 2009). For cell wall-modifying enzymes, this has been observed for PME enzyme activities during Arabidopsis seed germination (Müller et al., 2013). Whole-seed total PME activity increased until TR was reached and then declined. When ABA was added to the medium, TR still constituted the highest point of PME activity, but the activity only decreased with a delay after a plateau phase (Müller et al., 2013).

## Cell Wall-Modifying Enzymes Are Differentially Regulated at the Time of TR in Garden Cress in a Seed Compartment-Specific Manner

Cell wall modifications are necessary to allow radicle elongation and endosperm weakening, the two processes that eventually lead to ER (Schopfer, 2006; Linkies and Leubner-Metzger, 2012). It is also possible that cell wall modifications contribute to TR, as cell wall loosening in the RAD and CAP and a subsequent

in Figure 5. Note that the scales for CAP and RAD are different; note further that only intact CAPs (and corresponding RADs) were used at both time points. B to E, Normalized transcript abundances of selected group 2 PMEs. Seeds were imbibed without (control [CON]) or with ABA (5 $\mu$M). CAP and RAD were excised from seeds; results for CAP (left) and RAD (right) are displayed on identical scales. Early germination indicates seeds after TR but prior to ER (16 h). Late germination indicates seeds at $ER_{50\%}$, which was approximately 22 h for control treatment and approximately 65 h for ABA treatment. Only unruptured CAPs were sampled. *Lesa17210, Lesa04320,* and *Lesa20000* (Graeber et al., 2011) were used as references genes for the qRT-PCR normalization as described in "Materials and Methods." Mean values ± SE for four biological replicates are shown. The statistical significance of CAP and RAD results was analyzed separately by one-way ANOVA with Tukey's multiple comparison test performed using GraphPad Prism software (version 4.0; GraphPad Software; www.graphpad.com). Mean values labeled with different letters differ significantly from each other at $P < 0.05$.
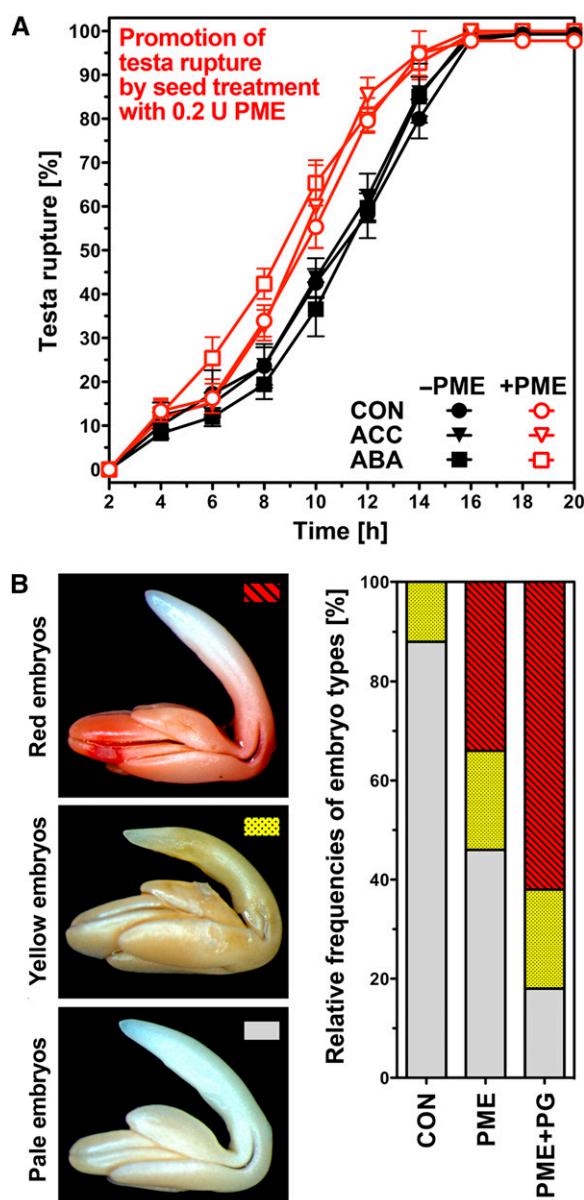
**Figure 8.** Treatment of garden cress seeds with low amounts of PME promotes TR and enhances testa permeability. A, Treatment of imbibed seeds with low amounts (0.2 units; i.e. 0.03 units mL⁻¹) of orange peel PME promoted but did not affect ER. This promotion of TR by low PME amounts was not affected by simultaneous treatment with ABA or ACC. Note that, in contrast to low amounts, relatively high amounts (approximately 20 units) of PME delayed TR and ER (Supplemental Fig. S5). Seeds were imbibed at 18°C in continuous light; mean values ± sᴇ of four biological replicates are shown. B, Treatment of seeds with PME and pectin degradation by PG enhances testa permeability as determined using the tetrazolium assay. Seeds were imbibed for 9 h in tetrazolium salt assay solution without (control [CON]) or with 0.2 units of PME or PME plus PG added. Embryos were excised and classified into five staining groups: pale (no staining, testa impermeable for tetrazolium salts), yellow (low testa permeability), and three categories of red (from partly to almost fully red; Supplemental Fig. S6). Relative numbers based on 50 embryos for each series are presented. For different subcategories of red-stained embryos, see Supplemental Figure S6. Red embryo staining is indicative for increased testa permeability.

volume increase through water uptake could provide the additional force necessary to overcome the breaking resistance of the testa. The testa is dead tissue, but cell wall-modifying enzymes could be secreted from the underlying endosperm to cause modifications in the inner testa cell walls, which could lead to site-specific weakening. A number of cell wall-modifying genes, and the enzyme activities of their products, have been shown to be differentially regulated before ER in the seeds of various endospermic species, such as β-1,3-glucanase in tobacco (*Nicotiana tabacum*; Leubner-Metzger et al., 1995; Manz et al., 2005), β-1,4-mannanase in tomato (*Solanum lycopersicum*; Nonogaki et al., 2000), garden cress (Morris et al., 2011), and Arabidopsis (Iglesias-Fernández et al., 2011), and xyloglucan endotransglycosylases/hydrolases in garden cress (Voegele et al., 2011; Graeber et al., 2014) and Arabidopsis (Endo et al., 2012), and species-specific changes in cell wall composition have been observed during the later germination process (Lee et al., 2012), supporting the importance of the cell wall remodeling during seed germination.

We found that PME activity during germination was 1 order of magnitude higher in the CAP than in the RAD. A higher activity in the seed-covering layers than the radicle was also observed in germinating seeds of the conifer yellow cypress (*Chamaecyparis nootkatensis* [formerly yellow cedar]; Ren and Kermode, 2000). We observed the highest PME activity in the garden cress CAP in the first hours after the start of imbibition (Fig. 5A), which possibly prevents preterm CAP weakening, similar to the observation by Müller et al. (2013) that high PME activity in whole seeds was associated with a delay of ER in Arabidopsis. Contrary to the CAP, the RAD showed an increase of PME activity only after TR.

Our modeling approach (Fig. 6) that used the CAP-and RAD-specific PME activities we measured as well as the compartment-specific transcriptomes predicted that group 2 PMEs, although they possess a PMEI domain, mainly contribute their PME activity, rather than an inhibitory effect on themselves or other PMEs, to the overall PME activity in the distinct seed compartments. Beyond seed, our mathematical modeling provides support with a completely independent approach for the experimental evidence provided by others (Wolf et al., 2009b) that the PMEI domains of group 2 PMEs are cleaved off during protein maturation and, thus, are not active as inhibitors.

## Changes in Pectin Methylesterification around TR Might Account for Transcriptome Changes through Mechanosensing Processes

In situ analyses indicated that deesterified HG was present throughout the garden cress seed cell walls during the whole germination process and was particularly abundant in the seed-covering layers, indicating that PMEs are widely active in seed cell walls. Me-HG

epitopes were only detected in the CAP around the time of TR. It is likely that this indicates the addition of new cell wall material in the endosperm, as there is currently no known mechanism by which methylester groups can be added to HG in muro. The fact that there are changes in PME activity as well as in the degree of methylesterification around the time of TR suggests that this contributes to the biomechanical changes that ultimately lead to ER (Linkies et al., 2009; Martínez-Andújar et al., 2012; Dekkers et al., 2013). It has been shown that changes in elasticity caused by changes in pectin methylesterification in the apical meristem are crucial for phyllotaxis (Peaucelle et al., 2011; Braybrook and Peaucelle, 2013). PME action also has been connected with brassinosteroid signaling, as several of the strong phenotypes caused by the overexpression of AtPMEI5 could be suppressed when a brassinosteroid receptor was mutated in the overexpressor (Wolf et al., 2012). Brassinosteroids are also known to promote germination in Arabidopsis (Steber and McCourt, 2001) and tobacco (Leubner-Metzger, 2001); thus, a change in their signaling caused by the regulation of PME activity might contribute to changes in germination behavior.

## Exposure to PMEs Changes Seed Coat Permeability and Germination Speed

Low levels of exogenous PME promoted TR and ER, while they was delayed by higher PME concentrations (Fig. 8). The opposing effects of different concentrations of PME might result from differences in the degree and pattern of demethylesterification caused by the different concentrations. It is possible that low PME concentrations accelerated water uptake and swelling of the seed due to increased seed coat permeability through cell wall loosening. Indeed, we found an increase in testa and/or mucilage permeability to tetrazolium in the presence of germination-accelerating concentrations of PME (Fig. 8). That this was a direct effect of the PME on the cell wall was demonstrated by a further increase in permeability when PG was also added. Treatment of garden cress seeds with the allelochemical myrigalone A increases the coat permeability (Voegele et al., 2012). In Arabidopsis, mutants with an increased testa permeability (transparent testa mutants) germinate faster than the wild type (Debeaujon et al., 2000). Moreover, methanol, which is released by PME action, is known to be a hydroxyl radical scavenger. Hydroxyl radicals have been shown to promote cell wall loosening associated with ER during garden cress seed germination (Müller et al., 2009). Hence, radical-mediated loosening of the CAP may be interfered with by the methanol produced through high PME activity, as would be expected from exposure to high concentrations of PME.

Altogether, on the basis of our findings, we conclude that garden cress seed germination entails tightly regulated changes in the degree of pectin methylesterification through seed compartment-specific differential expression of PMEs and PMEIs.

## MATERIALS AND METHODS

### Plant Material and Germination Kinetics

For all experiments, after-ripened seeds of garden cress (Lepidium sativum) 'FR14' were used (Graeber et al., 2010). Seeds were incubated in petri dishes with two layers of filter paper containing 6 mL of distilled and autoclaved water, sealed with Parafilm, and placed in a climate chamber with continuous light (approximately 100 $\mu$mol m$^{-2}$ s$^{-1}$) at 24°C for the microarrays and at 18°C for the PME experiments. TR and ER were scored at the indicated times. Where indicated, orange (Citrus sinensis) peel PME (P5400; Sigma), (+)cis-trans-ABA (Duchefa), or ACC (Sigma) was added in the indicated concentrations.

### RNA Extraction and Microarrays

Garden cress seed compartments (100 RADs, 100 CAPs, 200 NMEs, or 50 COTs) were homogenized in liquid nitrogen with a Precellys homogenizator for two cycles at 6,100 rpm, thawed in 1 mL of CTAB buffer (2% [w/v] hexadecyl-trimethyl-ammonium bromide, 2% [w/v] polyvinylpyrrolidone [molecular weight = 40,000], 100 mM Tris-HCl, pH 8, 25 mM EDTA, pH 8, 2 M NaCl, and 2% [v/v] $\beta$-mercaptoethanol), homogenized again, and then incubated at 65°C for 15 min. After two extraction steps with 1 mL of chloroform: isoamyl alcohol (24:1 [v/v]), the volume of the hydrophilic phase was determined, and one-fourth of that volume LiCl (10 M) was added. The RNA was precipitated at 4°C overnight. After centrifugation at 13,000 rpm and 4°C, the pellet was resuspended in 600 $\mu$L of SSTE buffer (1 M NaCl, 0.5% [w/v] SDS, 10 mM Tris-HCl, pH 8, and 1 mM EDTA), and two more chloroform extractions were performed in PhaseLock vials. The RNA was precipitated with sodium acetate/ethanol at −20°C, and the pellet was washed with ethanol, air dried, and resuspended in RNase-free water. An RNeasy column cleanup was performed according to the manufacturer's instructions including the optional DNase. The quality of the resulting RNA was assessed via nanodrop measurement, analytical gel electrophoresis, and integrity measurement on a bioanalyzer with a nanochip. RNAs were concentrated to 100 ng $\mu$L$^{-1}$ and shipped on dry ice to ServiceXS, which performed the antisense RNA synthesis and hybridizations to the Arabidopsis (Arabidopsis thaliana) GeneChip ATH1 Genome Array (Affymetrix).

### Probe Masking and Normalization

Masking determines how many probes of each probe set are retained in the analysis. The commonly used method for cross-species masking is to perform experiments hybridizing genomic DNA instead of RNA to the microarray and then masking probes whose DNA spot intensity is below an arbitrary cutoff (Hammond et al., 2005). This method assumes that any probe that shows a low binding signal in the DNA hybridization has no orthologous transcript of sufficient sequence similarity expressed in the species of interest, without taking into account that different probes have differing binding affinities. Instead, we performed an ANOVA on each probe individually to determine whether it is receiving signal or noise across conditions, allowing us to remove probes with no signal prior to normalization. To support that performing this ANOVA did not introduce an undesirable bias, most of the reference genes identified from Arabidopsis and garden cress seed transcriptomes (Graeber et al., 2011; Dekkers et al., 2012) have been kept in our masking process. To allocate the probes to probe sets before masking, the Arabidopsis custom chip definition file (CDF) from the CustomCDF project (Ath1121501_At_TAIRG.cdf v14.0.0; Dai et al., 2005) was used. This CDF maps the individual probes to their genes in Arabidopsis, using recent sequencing information from The Arabidopsis Information Resource (Lamesch et al., 2012); this eliminates the many-many relationship that exists in the original CDF. The probe-level spot intensities for all 107 chips, using the CustomCDF, were read into a matrix and were then normalized to have equal medians across each chip; this helps correct for the fact that the overall intensity of the chips varies prior to attempting to determine whether each probe represents signal. For each probe, a one-way ANOVA was used to test whether the mean expression across all conditions was the same, generating a $P$ value for each probe. A false discovery rate was then applied to these $P$ values, with threshold 0.01, to give a list of probes that show significant differences across the conditions. The probes that failed this test were removed from consideration, as were any probe sets with fewer than three probes remaining. To support that this ANOVA masking did not introduce an undesirable bias, of the 24 reference genes identified using Arabidopsis seed transcriptomes (Dekkers et al., 2012), all but one have been kept in our masking process. Furthermore, of the 15

reference gene candidates identified using the garden cress seed compartment-specific Complete Arabidopsis Transcriptome Microarray microarrays (Graeber et al., 2011), one is not on the ATH1 microarrays and nine were kept (Supplemental Fig. S7). These nine reference gene candidates include the three most stable reference genes for which the geometric mean was used for normalizing our qRT-PCR analysis; these were validated as being stable in the RNA samples used in this work. The chips were then background corrected and normalized using robust multiarray averaging (Irizarry et al., 2003) with the CDF resulting from the above masking method. The microarray data including the normalized intensity values for each microarray of our garden cress work were deposited in the National Center for Biotechnology Information's Gene Expression Omnibus with accession number GSE55702. Using the masking method presented here, with a false discovery rate of 0.01, 36.6% of probes and 65.1% of probe sets were retained, leading to 5,793 genes identified as being differentially expressed between 1 and 16 h after sowing in the CAP, and 6,098 genes in the RAD. Conversely, using the method of Hammond et al. (2005), the maximal number of differentially expressed genes was 1,712 at a cutoff of 100. Thus, our method retained a much larger number of differentially expressed genes that could then be used for further analysis.

## Immunofluorescence Microscopy

The preparation of plant materials and subsequent immunofluorescence microscopy with antibodies specific for specific cell wall epitopes were conducted as described (Lee et al., 2012).

## PME Activity Assay

Activity assays were performed as described (Downie et al., 1998) using esterified pectin from citrus fruit (P9561; Sigma) with more than 85% esterification with the following modifications: we used 4% (w/v) agarose, the incubation took place at 32°C, and after Ruthenium Red staining, an additional wash step was carried out overnight. For protein extraction, 100 RADs or 150 CAPs were ground in liquid nitrogen, and 200 $\mu$L of extraction buffer (40 mM sodium acetate, pH 5.2) was added. The samples were incubated on a shaker at 4°C for 10 min and then centrifuged at 10,000 rpm for 5 min at 4°C. For RADs and CAPs, 10 and 20 $\mu$L, respectively, of the supernatant were loaded directly into the wells of the agarose plate. For each time or treatment, three biological replicates were used. To normalize enzyme activities, protein concentration in the extracts was determined using the Bio-Rad Protein Assay Solution. A standard curve for PME activity was carried out with commercial pectinesterase from orange peel (P5400; Sigma). Stained zones on the agarose plates were analyzed with ImageJ software, and enzyme activity was calculated based on the standard curve (Supplemental Fig. S8).

## Mathematical Model of PME Activity in Seed Compartments

A model was developed to describe the action of PME and PMEIs in altering Me-HG into demethylesterified homogalacturonan. The two groups of PMEs (G1 and G2) and the PMEIs may form irreversible complexes (PMEI:G1 and PMEI:G2) as well as the self-inactivation of group 2 PMEs to form an inactive version (iG2). The PME demethylesterification rates of group $i$ PMEs is denoted $\alpha_i$, and the binding rates of the PMEI proteins with group $i$ PMEs are denoted $\zeta_i$. Group 2 PME molecules may inactivate themselves, in a unimolecular way, with binding rate $\zeta_3$, whereas the binding between PMEs and PMEIs is obviously bimolecular, as reflected in the nonlinear terms in Equations 1 to 8 (Fig. 6C). Transcript accumulation as measured from the microarrays for the two groups of PMEs and the PMEIs was used as a proxy for protein accumulation, with $\beta_p(t)$ being the production of the mRNA corresponding to protein $p$, and $C$ is a standardizing constant, to describe the relationship between protein and mRNA. To determine the values of the constants, the results from the model were fitted to the garden cress PME enzyme activity data for the RAD and CAP shown in Figure 5A using Matlab's genetic algorithm. The resulting PME activity predicted by the model after fitting is shown in Figure 6D. The resulting fitted parameters are shown in Supplemental Table S3.

## Testa Permeability Assay Using Tetrazolium

Entire garden cress seeds were incubated for 9 h in continuous light at 18°C with tetrazolium staining solution (Graeber et al., 2010; Voegele et al., 2012)

containing the indicated concentrations of PME (P5400; Sigma) or PG (17389; Sigma). The embryos were subsequently extracted, classified according to their staining intensity and patterns, and photographed.

## In Situ mRNA Hybridization

For *LesaPME11580*, a forward primer with an additional *Bam*HI restriction site (5′-ATGGATCCAGCAGTGACTGCAGCACCG-3′) and a reverse primer with an *Eco*RI site (5′-ATGAATTCCGTGTGAGTGTAGAGCGTGT-3′) were used to amplify a probe of 353 bp from reverse-transcribed RNA isolated from garden cress seeds. The probe spanned the pectinesterase domain. After digestion with *Bam*HI and *Eco*RI, the product was cloned into the pBluescript II KS+ vector. For the sense probe, the plasmid was linearized with *Xba*I and transcribed with T3 polymerase (Promega), while for the antisense probe, *Hind*III was used for linearization and T7 polymerase (Promega) was used for transcription with the digoxigenin labeling kit (Roche). Finally, the in situ hybridization was performed as described previously using 400 ng of probe per slide (Mayer et al., 1998).

## Sequence Alignments, Molecular Phylogenetic Analysis, and eNorthern Analysis

For all sequence and phylogenetic analyses, the bioinformatic software Geneious 5.0.4. (Biomatters) was used. Multiple sequence alignment on the basis of amino acid sequences of PMEs and PMEIs from different species was performed using the MUSCLE algorithm with default settings. For the phylogenetic tree, two different algorithms, MAFFT and MUSCLE, were used; two methods also were used for the tree construction, maximum likelihood (PHYML software) and Bayesian inference (MrBayes software). The eNorthern tool based on global transcriptome analysis of Arabidopsis at www.bar.utoronto.ca (Winter et al., 2007) was used for the visualization of transcript expression patterns of Arabidopsis PMEs and PMEI.

## Analyses of the Relative Transcript Abundance by qRT-PCR

cDNA synthesis and qRT-PCR were performed as described previously using *LesaG17210*, *LesaG20000*, and *LesaG04320* as reference genes (Graeber et al., 2011). Analysis of all raw data and calculation of the efficiency ($E$) and cycle threshold (CT) values were carried out with the PCR Miner software. The relative transcript abundance for every well was calculated as $(1 + E)^{-CT}$ and normalized against the geometric mean of the reference genes. The mean values of four biological replicates $\pm$ SE are shown. All primers were designed with the Geneious 5.0.4. software. Cloned cDNAs were sequenced and have been deposited as ESTs or full-length sequences to GenBank. Accession numbers and primer sequences are listed in Supplemental Table S4.

Sequence data from this article can be found in the GenBank/EMBL data libraries under accession numbers provided in Supplemental Table S4.

## Supplemental Data

The following supplemental materials are available.

**Supplemental Figure S1.** Cluster analysis of the garden cress differentially regulated transcriptome over time and seed compartments.

**Supplemental Figure S2.** Amino acid sequence alignment of garden cress PMEs and PMEIs.

**Supplemental Figure S3.** Spatial and temporal qRT-PCR analyses of PME and PMEI transcript abundances in germinating garden cress seeds.

**Supplemental Figure S4.** In situ mRNA hybridization detection of garden cress PME group 2 *LesaPME11580* transcripts.

**Supplemental Figure S5.** Effect of exogenous treatments of garden cress seeds with PME on TR and ER.

**Supplemental Figure S6.** Effect of exogenous treatments of garden cress seeds with PME and pectin degradation by PG on testa permeability.

**Supplemental Figure S7.** Expression of garden cress reference gene candidates.

**Supplemental Figure S8.** PME enzyme activity assay method.

**Supplemental Table S1.** Overrepresentation analysis of GO terms for CAP genes differentially up-regulated during TR.

**Supplemental Table S2.** Overrepresentation analysis of GO terms for RAD genes differentially up-regulated during TR.

**Supplemental Table S3.** Parameter values for the mathematical model.

**Supplemental Table S4.** GenBank accession numbers and primer sequences.

**Supplemental Data Set S1.** Normalized $\log_2$ expression values from individual microarrays for the garden cress seed compartments (13,895 transcripts).

**Supplemental Data Set S2.** Normalized $\log_2$ expression mean values for the garden cress seed compartments (13,895 transcripts).

**Supplemental Data Set S3.** Normalized $\log_2$ expression SD values for the garden cress seed compartments (13,895 transcripts).

**Supplemental Data Set S4.** Arabidopsis group 1 and 2 PMEs and PMEIs.

## LITERATURE CITED

**Bewley JD** (1997) Seed germination and dormancy. Plant Cell **9:** 1055–1066

**Braybrook SA, Hofte H, Peaucelle A** (2012) Probing the mechanical contributions of the pectin matrix: insights for cell growth. Plant Signal Behav **7:** 1037–1041

**Braybrook SA, Peaucelle A** (2013) Mechano-chemical aspects of organ formation in *Arabidopsis thaliana*: the relationship between auxin and pectin. PLoS ONE **8:** e57813

**Cosgrove DJ, Jarvis MC** (2012) Comparative structure and biomechanics of plant primary and secondary cell walls. Front Plant Sci **3:** 204

**Dai M, Wang P, Boyd AD, Kostov G, Athey B, Jones EG, Bunney WE, Myers RM, Speed TP, Akil H, et al** (2005) Evolving gene/transcript definitions significantly alter the interpretation of GeneChip data. Nucleic Acids Res **33:** e175

**Debeaujon I, Léon-Kloosterziel KM, Koornneef M** (2000) Influence of the testa on seed dormancy, germination, and longevity in Arabidopsis. Plant Physiol **122:** 403–414

**Dekkers BJ, Pearce S, van Bolderen-Veldkamp RP, Marshall A, Widera P, Gilbert J, Drost HG, Bassel GW, Müller K, King JR, et al** (2013) Transcriptional dynamics of two seed compartments with opposing roles in Arabidopsis seed germination. Plant Physiol **163:** 205–215

**Dekkers BJ, Willems L, Bassel GW, van Bolderen-Veldkamp RP, Ligterink W, Hilhorst HW, Bentsink L** (2012) Identification of reference genes for RT-qPCR expression analysis in Arabidopsis and tomato seeds. Plant Cell Physiol **53:** 28–37

**Downie B, Dirk LM, Hadfield KA, Wilkins TA, Bennett AB, Bradford KJ** (1998) A gel diffusion assay for quantification of pectin methylesterase activity. Anal Biochem **264:** 149–157

**Eckardt NA** (2005) VANGUARD1: at the forefront of pollen tube growth. Plant Cell **17:** 327–329

**Endo A, Tatematsu K, Hanada K, Duermeyer L, Okamoto M, Yonekura-Sakakibara K, Saito K, Toyoda T, Kawakami N, Kamiya Y, et al** (2012) Tissue-specific transcriptome analysis reveals cell wall metabolism, flavonol biosynthesis and defense responses are activated in the endosperm of germinating *Arabidopsis thaliana* seeds. Plant Cell Physiol **53:** 16–27

**Giovane A, Servillo L, Balestrieri C, Raiola A, D'Avino R, Tamburrini M, Ciardiello MA, Camardella L** (2004) Pectin methylesterase inhibitor. Biochim Biophys Acta **1696:** 245–252

**González-Carranza ZH, Elliott KA, Roberts JA** (2007) Expression of polygalacturonases and evidence to support their role during cell separation processes in *Arabidopsis thaliana*. J Exp Bot **58:** 3719–3730

**Graeber K, Linkies A, Müller K, Wunchova A, Rott A, Leubner-Metzger G** (2010) Cross-species approaches to seed dormancy and germination: conservation and biodiversity of ABA-regulated mechanisms and the Brassicaceae *DOG1* genes. Plant Mol Biol **73:** 67–87

**Graeber K, Linkies A, Steinbrecher T, Mummenhoff K, Tarkowská D, Turečková V, Ignatz M, Sperber K, Voegele A, de Jong H, et al** (2014) Delay of germination 1 mediates a conserved coat-dormancy mechanism for the temperature- and gibberellin-dependent control of seed germination. Proc Natl Acad Sci USA **111:** E3571–E3580

**Graeber K, Linkies A, Wood ATA, Leubner-Metzger G** (2011) A guideline to family-wide comparative state-of-the-art quantitative RT-PCR analysis exemplified with a Brassicaceae cross-species seed germination case study. Plant Cell **23:** 2045–2063

**Hammond JP, Bowen HC, White PJ, Mills V, Pyke KA, Baker AJM, Whiting SN, May ST, Broadley MR** (2006) A comparison of the *Thlaspi caerulescens* and *Thlaspi arvense* shoot transcriptomes. New Phytol **170:** 239–260

**Hammond JP, Broadley MR, Craigon DJ, Higgins J, Emmerson ZF, Townsend HJ, White PJ, May ST** (2005) Using genomic DNA-based probe-selection to improve the sensitivity of high-density oligonucleotide arrays when applied to heterologous species. Plant Methods **1:** 10

**Hyodo H, Terao A, Furukawa J, Sakamoto N, Yurimoto H, Satoh S, Iwai H** (2013) Tissue specific localization of pectin-$Ca^{2+}$ cross-linkages and pectin methyl-esterification during fruit ripening in tomato (Solanum lycopersicum). PLoS ONE **8:** e78949

**Iglesias-Fernández R, Rodríguez-Gacio MC, Barrero-Sicilia C, Carbonero P, Matilla A** (2011) Three endo-$\beta$-mannanase genes expressed in the micropylar endosperm and in the radicle influence germination of Arabidopsis thaliana seeds. Planta **233:** 25–36

**Irizarry RA, Hobbs B, Collin F, Beazer-Barclay YD, Antonellis KJ, Scherf U, Speed TP** (2003) Exploration, normalization, and summaries of high density oligonucleotide array probe level data. Biostatistics **4:** 249–264

**Lamesch P, Berardini TZ, Li D, Swarbreck D, Wilks C, Sasidharan R, Muller R, Dreher K, Alexander DL, Garcia-Hernandez M, et al** (2012) The Arabidopsis Information Resource (TAIR): improved gene annotation and new tools. Nucleic Acids Res **40:** D1202–D1210

**Lee KJD, Dekkers BJW, Steinbrecher T, Walsh CT, Bacic A, Bentsink L, Leubner-Metzger G, Knox JP** (2012) Distinct cell wall architectures in seed endosperms in representatives of the Brassicaceae and Solanaceae. Plant Physiol **160:** 1551–1566

**Leubner-Metzger G** (2001) Brassinosteroids and gibberellins promote tobacco seed germination by distinct pathways. Planta **213:** 758–763

**Leubner-Metzger G, Fründt C, Vögeli-Lange R, Meins F Jr** (1995) Class I ß-1,3-glucanases in the endosperm of tobacco during germination. Plant Physiol **109:** 751–759

**Linkies A, Leubner-Metzger G** (2012) Beyond gibberellins and abscisic acid: how ethylene and jasmonates control seed germination. Plant Cell Rep **31:** 253–270

**Linkies A, Müller K, Morris K, Turecková V, Wenk M, Cadman CSC, Corbineau F, Strnad M, Lynn JR, Finch-Savage WE, et al** (2009) Ethylene interacts with abscisic acid to regulate endosperm rupture during germination: a comparative approach using *Lepidium sativum* and *Arabidopsis thaliana*. Plant Cell **21:** 3803–3822

**Liu PP, Koizuka N, Martin RC, Nonogaki H** (2005) The BME3 (Blue Micropylar End 3) GATA zinc finger transcription factor is a positive regulator of Arabidopsis seed germination. Plant J **44:** 960–971

**Manz B, Müller K, Kucera B, Volke F, Leubner-Metzger G** (2005) Water uptake and distribution in germinating tobacco seeds investigated in vivo by nuclear magnetic resonance imaging. Plant Physiol **138:** 1538–1551

**Markovic O, Janecek S** (2004) Pectin methylesterases: sequence-structural features and phylogenetic relationships. Carbohydr Res **339:** 2281–2295

**Martínez-Andújar C, Pluskota WE, Bassel GW, Asahina M, Pupel P, Nguyen TT, Takeda-Kamiya N, Toubiana D, Bai B, Górecki RJ, et al** (2012) Mechanisms of hormonal regulation of endosperm cap-specific gene expression in tomato seeds. Plant J **71:** 575–586

**Mayer KF, Schoof H, Haecker A, Lenhard M, Jürgens G, Laux T** (1998) Role of WUSCHEL in regulating stem cell fate in the Arabidopsis shoot meristem. Cell **95:** 805–815

**Mohnen D** (2008) Pectin structure and biosynthesis. Curr Opin Plant Biol **11:** 266–277

**Morris K, Linkies A, Müller K, Oracz K, Wang X, Lynn JR, Leubner-Metzger G, Finch-Savage WE** (2011) Regulation of seed germination in the close Arabidopsis relative *Lepidium sativum*: a global tissue-specific transcript analysis. Plant Physiol **155:** 1851–1870

**Müller K, Levesque-Tremblay G, Bartels S, Weitbrecht K, Wormit A, Usadel B, Haughn G, Kermode AR** (2013) Demethylesterification of cell wall pectins in Arabidopsis plays a role in seed germination. Plant Physiol **161:** 305–316

**Müller K, Linkies A, Vreeburg RAM, Fry SC, Krieger-Liszkay A, Leubner-Metzger G** (2009) In vivo cell wall loosening by hydroxyl radicals during cress seed germination and elongation growth. Plant Physiol **150:** 1855–1865

**Müller K, Tintelnot S, Leubner-Metzger G** (2006) Endosperm-limited Brassicaceae seed germination: abscisic acid inhibits embryo-induced endosperm weakening of *Lepidium sativum* (cress) and endosperm rupture of cress and *Arabidopsis thaliana*. Plant Cell Physiol **47:** 864–877

**Nonogaki H, Gee OH, Bradford KJ** (2000) A germination-specific endo-β-mannanase gene is expressed in the micropylar endosperm cap of tomato seeds. Plant Physiol **123:** 1235–1246

**Peaucelle A, Louvet R, Johansen JN, Salsac F, Morin H, Fournet F, Belcram K, Gillet F, Höfte H, Laufs P, et al** (2011) The transcription factor BELLRINGER modulates phyllotaxis by regulating the expression of a pectin methylesterase in Arabidopsis. Development **138:** 4733–4741

**Pelletier S, Van Orden J, Wolf S, Vissenberg K, Delacourt J, Ndong YA, Pelloux J, Bischoff V, Urbain A, Mouille G, et al** (2010) A role for pectin de-methylesterification in a developmentally regulated growth acceleration in dark-grown Arabidopsis hypocotyls. New Phytol **188:** 726–739

**Pelloux J, Rustérucci C, Mellerowicz EJ** (2007) New insights into pectin methylesterase structure and function. Trends Plant Sci **12:** 267–277

**Ren C, Kermode AR** (2000) An increase in pectin methyl esterase activity accompanies dormancy breakage and germination of yellow cedar seeds. Plant Physiol **124:** 231–242

**Saez-Aguayo S, Ralet MC, Berger A, Botran L, Ropartz D, Marion-Poll A, North HM** (2013) PECTIN METHYLESTERASE INHIBITOR6 promotes *Arabidopsis* mucilage release by limiting methylesterification of homo-galacturonan in seed coat epidermal cells. Plant Cell **25:** 308–323

**Schopfer P** (2006) Biomechanics of plant growth. Am J Bot **93:** 1415–1425

**Slotte T, Holm K, McIntyre LM, Lagercrantz U, Lascoux M** (2007) Differential expression of genes important for adaptation in *Capsella bursa-pastoris* (Brassicaceae). Plant Physiol **145:** 160–173

**Steber CM, McCourt P** (2001) A role for brassinosteroids in germination in Arabidopsis. Plant Physiol **125:** 763–769

**Tan L, Eberhard S, Pattathil S, Warder C, Glushka J, Yuan C, Hao Z, Zhu X, Avci U, Miller JS, et al** (2013) An Arabidopsis cell wall proteoglycan consists of pectin and arabinoxylan covalently linked to an arabinogalactan protein. Plant Cell **25:** 270–287

**Thompson DS** (2005) How do cell walls regulate plant growth? J Exp Bot **56:** 2275–2285

**Voegele A, Graeber K, Oracz K, Tarkowská D, Jacquemoud D, Turečková V, Urbanová T, Strnad M, Leubner-Metzger G** (2012) Embryo growth, testa permeability, and endosperm weakening are major targets for the environmentally regulated inhibition of *Lepidium sativum* seed germination by myrigalone A. J Exp Bot **63:** 5337–5350

**Voegele A, Linkies A, Müller K, Leubner-Metzger G** (2011) Members of the gibberellin receptor gene family *GID1* (*GIBBERELLIN INSENSITIVE DWARF1*) play distinct roles during *Lepidium sativum* and *Arabidopsis thaliana* seed germination. J Exp Bot **62:** 5131–5147

**Wakabayashi K, Chun JP, Huber DJ** (2000) Extensive solubilization and depolymerization of cell wall polysaccharides during avocado (*Persea americana*) ripening involves concerted action of polygalacturonase and pectinmethylesterase. Physiol Plant **108:** 345–352

**Wakabayashi K, Hoson T, Huber DJ** (2003) Methyl de-esterification as a major factor regulating the extent of pectin depolymerization during fruit ripening: a comparison of the action of avocado (*Persea americana*) and tomato (*Lycopersicon esculentum*) polygalacturonases. J Plant Physiol **160:** 667–673

**Wang M, Yuan D, Gao W, Li Y, Tan J, Zhang X** (2013) A comparative genome analysis of PME and PMEI families reveals the evolution of pectin metabolism in plant cell walls. PLoS ONE **8:** e72082

**Willats WGT, McCartney L, Mackie W, Knox JP** (2001) Pectin: cell biology and prospects for functional analysis. Plant Mol Biol **47:** 9–27

**Winter D, Vinegar B, Nahal H, Ammar R, Wilson GV, Provart NJ** (2007) An "Electronic Fluorescent Pictograph" browser for exploring and analyzing large-scale biological data sets. PLoS ONE **2:** e718

**Wolf S, Mouille G, Pelloux J** (2009a) Homogalacturonan methyl-esterification and plant development. Mol Plant **2:** 851–860

**Wolf S, Mravec J, Greiner S, Mouille G, Höfte H** (2012) Plant cell wall homeostasis is mediated by brassinosteroid feedback signaling. Curr Biol **22:** 1732–1737

**Wolf S, Rausch T, Greiner S** (2009b) The N-terminal pro region mediates retention of unprocessed type-I PME in the Golgi apparatus. Plant J **58:** 361–375

**Yang XY, Zeng ZH, Yan JY, Fan W, Bian HW, Zhu MY, Yang JL, Zheng SJ** (2013) Association of specific pectin methylesterases with Al-induced root elongation inhibition in rice. Physiol Plant **148:** 502–511

**Yoshida S, Barbier de Reuille P, Lane B, Bassel GW, Prusinkiewicz P, Smith RS, Weijers D** (2014) Genetic control of plant development by overriding a geometric division rule. Dev Cell **29:** 75–87